CHEMICAL ENGINEERING TRANSACTIONS
VOL. 109, 2024
A publication of AIDIC
The Italian Association of Chemical Engineering
Online at www.cetjournal.it
Guest Editors: Leonardo Tognotti, Rubens Maciel Filho, Viatcheslav Kafarov
Copyright © 2024, AIDIC Servizi S.r.l.
ISBN 979-12-81206-09-0; **ISSN** 2283-9216
DOI: 10.3303/CET24109105

Hydrothermal Synthesis and Photocatalytic Properties of $CaTiSiO_5$ for Hydrogen Production

Ulises Arellano[b], Lifang Chen[a,*], Jin An Wang[a], José Salmones[a], Roberto Limas[a], Luis E. Noreña[c,], Silvia Solís[d], Victor H. Lara[d]

[a]Escuela Superior de Ingeniería Química e Industrias Extractivas, Instituto Politécnico Nacional, Col. Zacatenco, 07738, Ciudad de México, Mexico
[b]Colegio de Ciencias y Humanidades, Universidad Autónoma de la Ciudad de México, 09620 Ciudad de México, Mexico
[c]Departamento de Ciencias Básicas, Universidad Autónoma Metropolitana-AzcapotzalcoCiudad de México, Mexico.
[d]Departamento de Química, Universidad Autónoma Metropolitana-Iztapalapa, Iztapalapa, 09430 Ciudad de México, Mexico
lchen@ipn.mx

Titanite ($CaTiSiO_5$) nanomaterials were synthesized by two hydrothermal methods and then calcined at 550 and 1000 °C, respectively. Their textural properties, crystalline structures, morphological features, and optical properties were characterized using N_2 adsorption-desorption isotherms (BET), X-ray diffraction (XRD), transmission electron microscopy-energy dispersive spectroscopy (TEM-EDS), thermogravimetry-differential thermal analysis (TG-DTA), and UV-vis spectroscopy. The samples calcined at 550 °C mainly consisted of anatase TiO_2 with some $CaCO_3$ and amorphous SiO_2, which converted into $CaTiSiO_5$ with a small amount of $CaSiO_3$ at 1000 °C. The band gap energy (E_g) was lower because of the $CaTiSiO_5$ formation at higher calcination temperature. The $CaTiSiO_5$ photoactivity was evaluated in water splitting under UV light irradiation for H_2 production. The highest H_2 production rate was obtained with the nanomaterials prepared by the Method II calcined at 1000 ºC. When formic acid was used as sacrificial agent, the hydrogen generation rate remarkably increased by 3 - 5 times (160 $\mu mol \cdot g^{-1} \cdot h^{-1}$). However, in the presence of methanol, the hydrogen generation rate was not significantly increased. Clearly, the acidic reaction media promoted the reduction of protons on the surface of the catalysts by trapping the excited electrons in the $CaTiSiO_5$ conduction band, favouring the hydrogen production.

1. Introduction

The rapid growth in world population and industrial activities has led to energy consumption increasing and serious environmental challenges. The utilization of the non-renewable fossil fuels produces a great amount of greenhouse gases and air pollutants, causing irreversible damage to the global environment. In the research for new energy sources, scientists have proposed various technical routes, notably the hydrogen utilization [Maeda K., 2011]. Hydrogen is an alternative fuel to meet energy demands and reduce global pollutants, and hence, it is friendly to the environment. Hydrogen is abundant in various renewable sources. However, hydrogen is not a primary energy source and it needs particular transformation processes. A variety of hydrogen production techniques, such as hydrocarbon dehydrogenation, catalytic decomposition of natural gas, and water electrolysis have been developed [Zhu J. and Zäch M., 2009].
Currently, the photocatalytic technique is widely investigated for hydrogen production where the photocatalysts take the key role. Titanite is known as a silicate of titanium and calcium mineral which belongs to the group of silicates [Muthuraman M. and Patil K. C., 1998]. The crystal structure of titanite ($CaTiSiO_5$) consists of a corner-sharing [TiO_6] octahedron, an isolated [SiO_4] tetrahedron, and an irregular sevenfold coordination [CaO_7].
The [TiO_6] octahedron is joined by the corners and forms chains along the *a* direction and is interconnected by the [SiO_4] tetrahedron and the [CaO_7] polyhedron [Stoyanova T. et al., 2017]. Normally, the pure titanite is colourless, but it turns colourful when doped with transition metals, which may act as chromophore material [Zhu J., Zäch M., 2009].

Paper Received: 19 March2024 ; Revised: 6 April 2024; Accepted: 22 May 2024
Please cite this article as: Arellano U., Chen L., Wang J.A., Salmones J., Limas R., Noreña L.E., Solís S., Lara V.H., 2024, Hydrothermal Synthesis and Photocatalytic Properties of Catisio5 for Hydrogen Production, Chemical Engineering Transactions, 109, 625-630 DOI:10.3303/CET24109105

Therefore, titanite possesses interesting optical properties and has potential to be used as photomaterials. However, $CaTiSiO_5$ used as photocatalyst for hydrogen production via water splitting has not been reported yet. In the present work, titanite solids was synthesized by the hydrothermal method, and for the first time, it was used as photocatalyst for hydrogen production via water splitting under ultra-visible (UV) irradiation. The effect of the calcination temperature, 550 and 1000 °C, on the crystalline structure and optical properties, and the titanite photoactivity was investigated. The effect of formic acid and methanol as sacrificial reagents on the hydrogen generation rate was also evaluated.

2. Experimental procedure

2.1 Synthesis of titanite

Method I: A solution consisting of tetraethyl orthosilicate (TEOS), methanol and water with a 1:1:1 molar ratio, was prepared under magnetic stirring at room temperature. Another $CaCl_2$ solution (3.4×10^{-3} M) was prepared using deionized water and $CaCl_2{\cdot}H_2O$ (Sigma, 99%). Separately, a third solution was prepared with a 1:1 molar ratio of titanium isopropoxide and 2-propanol. The second and third solutions were slowly dropped into the TEOS solution, to form a mixture under stirring. Afterwards, a solution of H_2O, Triton-X 100, and HCl with a $0.2:1.7\times10^{-4}:2\times10^{-3}$ molar ratio was added into the previous resulting mixture under stirring for 60 min. The suspended mixture was transferred into a Teflon bottle that was tightly sealed and kept at 120 °C for 72 h of hydrothermal treatment. The resulting material was washed with deionized water and dried at 80 °C for 12h. The dried solids were divided into two parts, one part was calcined at 550 °C for 6 h, and the rest was calcined at 1000 °C for 6 h, in an oven with a temperature raising rate of 1 °C/min.
Method II: A solution of TEOS, methanol and water with a molar ratio of 1:4:0.5 was prepared under stirring for 20 min at room temperature. A second solution was prepared using titanium (IV) isopropoxide and 2-propanol at a 1:2 molar ratio under 20 min of stirring at room temperature. These two solutions were mixed by dropping the titanium solution into the TEOS solution. Then, 0.01 M of HCl and 1 M $CaCl_2$ solution was added. The resulting mixture was stirred for 60 min, and then kept for 24 h. Separately, a 2% w/v Triton-X100 solution was added dropwise to the initial alkoxide solution until a 20% v/v was obtained. In this stage, the suspended mixture was stirred for 24 h at room temperature. Finally, the above mixture was hydrothermally treated inside a Teflon bottle at 120 °C for 120 h. The resulting material was washed, dried and calcined as described above.
The materials obtained by the two synthesis methods were labeled as: CaTiSi-I-550, CaTiSi-I-1000, CaTiSi-II-550, and CaTiSi-II-1000, where numbers I and II represent Method I and Method II, respectively; 550 and 1000 are the calcination temperatures in °C; and Ca, Ti and Si represent the calcium, titanium, and silicon elements in the titanite solids, respectively.

2.2 Characterization

The textural properties of the samples were measured by the N_2 physisorption method on a Micromeritics ASAP 2000 analyzer. The morphology of the solids was observed by transmission electron microscopy (TEM) on a JEOL 2100F instrument, using 200 kV acceleration as illumination source. The TEM instrument was coupled with an X-ray energy dispersive spectroscopy (EDS) analyzer for surface chemical composition determination of the selected area. The X-ray diffractograms (XRD) were obtained using a Siemens D500 diffractometer coupled to a tube with copper anode using Cu kα radiation (λ=1.5406 Å), 35 kV and 20 mA. The thermogravimetry-differential thermal analysis (TG-DTA) was carried out on a Perkin Elmer Analyzer TGA/DTA equipment, Diamond model. The UV-vis diffuse reflectance spectra were obtained using an Evolution-220 spectrometer (Thermo Fisher Scientific).

2.3 Photoactivity measurement

We employed a Pyrex reaction cell connected to a closed gas circulation and a vacuum system for photoactivity measurement. 50 mg of the photocatalyst powders were dispersed in the cell containing 200 mL of the reaction mixture (the volume ratio of sacrificial agent to water was 1:1). Prior to reaction, the mixture was sparged with nitrogen for 5 min to remove the air inside, and it was subsequently irradiated with a 2.16 W UV lamp (UVP Pen Ray lamp, 18 mA intensity 2.5 mW/cm^2, λ = 254 nm) protected by a quartz tube. The gaseous products were periodically analyzed by a Shimadzu GC-8A on-line gas chromatograph analyzer, equipped with a thermal conductivity detector (TCD) and a packed Shincarbon column (2 m length, 1mm I.D. and 2.5mm O.D.). The gas chromatograph (GC) operating conditions were as follows: column temperature 40 °C, injector temperature 60 °C, detector temperature 60 °C, and a current intensity in the detector filament of 60 mA. Nitrogen (99.9%) was used as carrier.

3. Results and discussion

3.1 XRD analysis

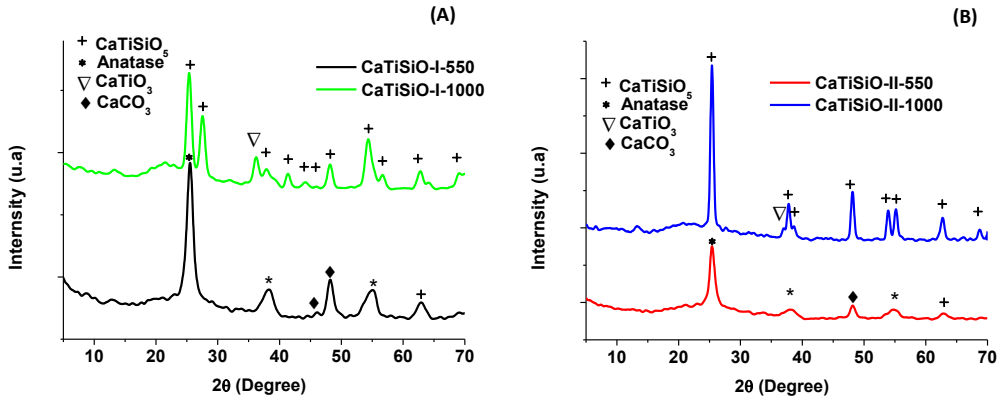

Figure 1: XRD patterns of $CaTiSiO_5$ materials calcined at different temperatures. (A) Method I; (B) Method II.

Figure 1 shows the XRD patterns of the $CaTiSiO_5$ nanomaterials. For the sample prepared by Method I and calcined at 550 °C, TiO_2 phase (anatase) and was mainly formed, indicated by the most intense diffraction signals at 2θ angles of 25.1°, which corresponds to the reflection of the (101) plane of TiO_2 anatase crystals, [Wang J.A. et al, 2001]. A small amount of wollastonite ($CaSiO_3$) and calcite $CaCO_3$ were also present, assigned to the intermediate phases prior to titanite ($CaTiSiO_5$) formation. No signals of the coesite phase (SiO_2) were observed because of its amorphous characteristics [Muthuraman M. et al, 2017]. By increasing the calcination temperature to 1000 °C, the solid-state reactions amongst TiO_2, SiO_2, $CaSiO_3$ or $CaCO_3$ phases formed $CaTiSiO_5$ [Downs R.T. and Hall-Wallace M., 2003], according to the following reactions (1) and (2) [Li Z., et al., 2017]:

$$CaSiO_3 + TiO_2 \rightarrow CaTiSiO_5 \quad (1)$$

$$CaCO_3 + SiO_2 + TiO_2 \rightarrow CaTiSiO_5 + CO_2 \uparrow \quad (2)$$

For the solid synthesized by Method II, at a 550 °C calcination temperature, anatase TiO_2 and $CaCO_3$ were formed. At 1000 °C calcination, the main diffraction peaks were indexed to the $CaTiSiO_5$ phase. In sum, at 550 °C calcination, a mixture of different phases was obtained by these two synthetic methods; at 1000 °C calcination, Method-I led to formation of titanite as major and $CaTiO_3$ as minor. Method-II led to almost pure titanite with large crystallites.

3.2 TG/DTA analysis

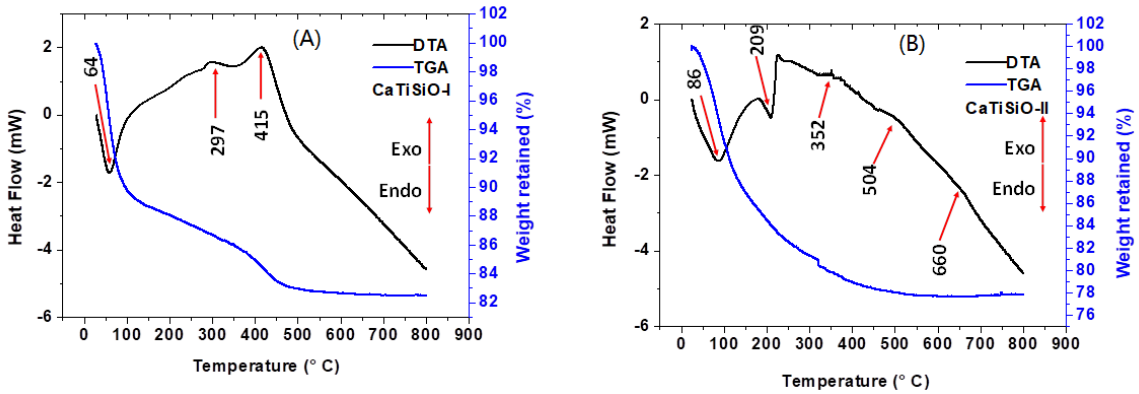

Figure 2: TGA-DTA profiles of the fresh $CaTiSiO_5$ solids (A) Method-I; (B) Method-II

Figure 2A shows the thermal analysis of the fresh (CaTiSi-I) nanomaterial prepared by Method I. The TG curve presents two weight loss stages in the temperature ranges of 26-320 °C, and 320-550 °C, respectively. Accordingly, there are two endothermic peaks in the DTA curve within this range. The weight loss (approximately 13wt%) in the first stage (26-320 °C), was attributed to the desorption of physisorbed H_2O and the decomposition

of hydroxide or hydrogel materials. The second stage of weight loss (approximately 4wt%) with a strong exothermic signal at 415 °C was assigned to the release of CO_2 due to the combustion of organic residues. Above 550 °C, no weight loss in the TG curve was observed; however, the DTA curve continuously declined, indicating the formation of the titanite phase ($CaTiSiO_5$) via the solid-state reaction between $CaSiO_3$ and TiO_2. Similarly, in Figure 2B, there are two endothermic peaks between 26 and 300 °C, accompanying around 18 wt% of weight loss, which was assigned to the release of adsorbed water and the decomposition of hydroxide or hydrogels. The second weight loss (4 wt%) appeared between 300 and 550 °C, accompanied by two exothermic peaks, which were assigned to the combustion of organic residues. Above 600 °C, no weight loss was observed but heat release still was taking place, indicating $CaTiSiO_5$ formation by the solid-state reactions [Thomas M. and Michael F. 2018]. This could be associated with the crystallization of more than one phase or a transformation process, such as $CaTiSiO_5$ undergoing a phase transition from a low-temperature monoclinic P21/a phase to a high-temperature monoclinic A2/a phase, accompanied by the displacements of Ti atoms from their off-center position to the center of the TiO_6 octahedra [Stoyanova T., et al 2009].

3.3. Morphological features and element analysis

Figure 3 shows the TEM micrographs and EDS spectra of the nanomaterials. Increasing the calcination temperature from 550 to 1000 °C led to large crystals formation in the nanomaterial. All the four materials had a composition of Si, Ca, Ti, and O elements in the selected area, indicating the homogeneity of the nanomaterials.

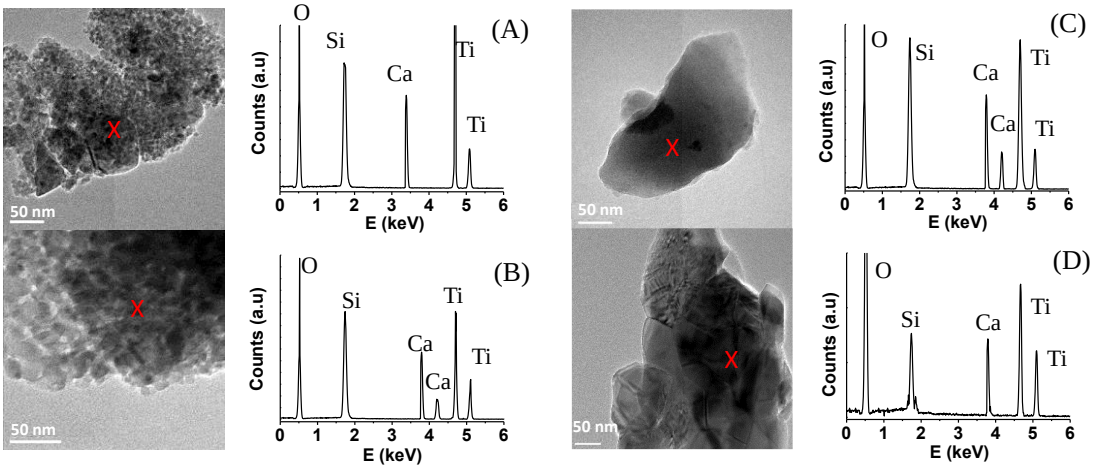

Figure 3. TEM micrographs and EDS profiles of the $CaTiSiO_5$ materials.
(A): CaTiSiO-I-550; (B): CaTiSiO-II-550; (C) CaTiSiO-I-1000; (D) CaTiSiO-II-1000.

3.4. Photoactivity for H_2 generation

Figure 4A shows the UV-vis diffuse reflectance spectra of the $CaTiSiO_5$ nanomaterials. The UV-absorption bands at around 225 nm, 272 nm, and 320 nm were principally assigned to the ligand-to-metal charge transfer of $O^{2-} \rightarrow Ti^{4+}$, and $Ti^{3+} \rightarrow Ti^{4+}$ in TiO_2 or $CaTiSiO_5$ [Mahanta U, et al. 2022]. The values of the forbidden band energy (E_g) were calculated by the T_{auc} method [O'Leary S.K. and Lim P.K., 1997]. The E_g values of the materials calcined at 1000 °C were 2.8-2.9 eV which are smaller than the 3.15 eV value obtained at 550 °C. Figure 4B shows the amount of H_2 produced under UV light irradiation using formic acid as sacrificial agent. An increase in the amount of H_2 generated was observed by increasing the calcination temperature of the catalysts. The most active CaTiSi-II-1000 catalyst can produce approximately 800 $\mu molg^{-1}$ of hydrogen after 5h of reaction. The photoactivity of the materials calcined at 550 °C (CaTiSi-I-550 and CaTISi-II-550) are relatively similar for the two synthesis methods. The photocatalytic activity increased according to the following order:

CaTiSi-II-1000 > CaTISi-I-1000 > CaTiSi-I-550 ~ CaTISi-II-550 (3)

The above catalytic behaviors are related to the synthetic method, the calcination temperature, and the phase composition. At the calcination temperature 1000 °C, $CaTiSiO_5$ phase dominates in nanomaterials, which is more active for water photo-splitting due to its lower E_g value. Particularly, the nanomaterial synthesized by Method II consists of almost pure $CaTiSiO_5$ at 1000 °C, therefore, it shows the highest photocatalytic activity. Figure 4C shows the hydrogen generation rate of the catalysts under UV light radiation in the absence of sacrificial agent (standard) and in the presence of sacrificial agents (methanol and formic acid). Without a

sacrificial agent, the H_2 generation rate was lower than 41 μmol $g^{-1}h^{-1}$, depending of the catalysts. In the presence of methanol as sacrificial agent, the H_2 generation rate was increased by approximately by 40-50%. However, using formic acid as sacrificial agent, the H_2 generation rate was significantly increased by 3 - 5 times in comparison with that achieved under the standard condition. The addition of a sacrificial agent inhibited the electron-hole pair recombination rate and improved the photocatalytic activity for H_2 production [Fontelles O., et al, 2018]. The nanomaterials that absorbed the UV light energy produced a large number of holes by separating the e^-/h^+ pairs. The holes may oxidize the sacrificial agents and produced more protons; while, the excited electrons favored the reduction of protons to H_2, according to the reactions 4 to 7 [Udani P. P. C., Rønning M., 2015].

$$CaTiSiO_5 + h\nu \rightarrow CaTiSiO_5 + h^+ + e^- \quad (4)$$

$$h\nu + H_2O_{ads} \rightarrow OH^- + H^+ \quad (5)$$

$$CH_3OH_{ads} + h^+(OH) \rightarrow CO_2 + H^+ (H_2O) \quad (6)$$

$$2H^+ + 2e^- \rightarrow H_2 \quad (7)$$

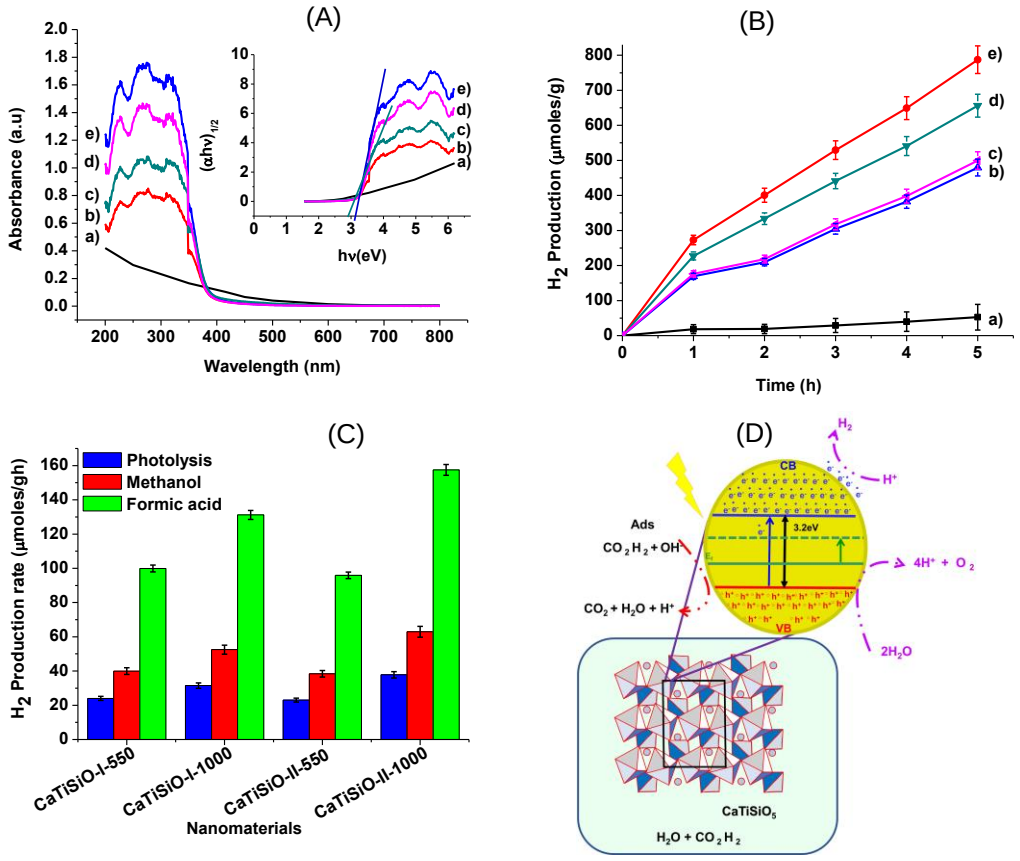

Figure 4. (A) UV-vis diffuse reflectance spectra of $CaTiSiO_5$ materials and the $[F(R)\ h\nu]^2$ as a function of $h\nu$ (inset); (B) H_2 production amount with different catalysts in the presence of UV-vis light irradiation. Catalyst mass: 0.05 g; sacrificial agent: formic acid. (C) H_2 production rate under different conditions and catalyst; (D) A proposed H_2 generation mechanism on the surface of titanite catalysts in the presence of formic acid. (a): Photolysis; (b) CaTiSiO-II-550; (c) CaTiSiO-I-550; (d) CaTiSiO-I-1000; (e) CaTiSiO-II-1000.

Under UV light irradiation, titanite absorbs electromagnetic energy to generate electron-hole pairs (e^- - h^+). The excited electrons can jump from the valence band (VB) to the conduction band (CB), leaving the h^+ in the VB layer. The surface adsorbed CH_3OH may be oxidized to CO_2 by the positively charged holes; and protons are capable of capturing the photogenerated mobile electrons in the CB to form H_2. Usually, the amount of photoproduced H_2 by water splitting is rather small, due to the holes and electrons recombination effect. For this reason, it is necessary to use some sacrificial agents to irreversibly consume the photogenerated holes, inhibiting the charges recombination rate and increasing the H_2 production efficiency. The H_2 generation mechanism on the surface of titanite in the presence of formic acid was pictured in Figure 4D.

In the absence of a sacrificial agent in the reaction medium, the pH value of water is approximately 7. As formic acid was added, the reaction media became acidic (pH = 4). On the other hand, methanol addition led to a basic reaction medium (pH = 9). Under a basic condition, although H_2 production is not inhibited, methanol adsorption on the surface of the catalyst gave rise to the formation of new surface functional groups that do not favor the generation of radicals for the dissociation of water [Chen J. and Ollis D.F., 1999]. The H_2 production rate was greatly enhanced when formic acid was used as sacrificial agent, due to the high protons surface concentration in an acid media [Chiarello G. L., et al, 2018]. In comparison with the H_2 generation rate achieved on TiO_2 (22.3 μmol $g^{-1}h^{-1}$), TiO_2-ZrO_2 (53.4 μmol $g^{-1}h^{-1}$), and 0.75wt%Ag/TiO_2-ZrO_2 (140 μmol $g^{-1}h^{-1}$) under similar condition, our $CaTiSiO_5$-II-1000 catalyst (160 μmol $g^{-1}h^{-1}$) exhibited a higher photoactivity [Onsuratoom, S. et al., 2011].

4. Conclusions

Ternary titanite ($CaTiSiO_5$) solids were synthesized by two hydrothermal methods. These materials have a mesoporous texture with E_g values in the range of 3.2 to 2.8 eV. The $CaTiSiO_5$ calcined at 1000 ºC shows a lower E_g value and a high photoactivity for the production of hydrogen under UV irradiation. The H_2 generation rate was greatly enhanced by 3-4 times (160 μmol $g^{-1}h^{-1}$) when formic acid was added as sacrificial agent in the reaction mixture. Formic acid addition not only lowered the pH value of the reaction mixture but also diminished the concentration of holes in the surface of the catalysts, thus inhibiting the recombination of the e^-/h^+ pairs and enhancing the hydrogen generation rate. In the near future, the structural doping of $CaTiSiO_5$ nanomaterials will be performed to further decreasing the band gap energies in order to investigate the water photo-splitting activity under visible light region.

Acknowledgments

Dr. Lifang Chen thanks the financial support from the Instituto Politécnico Nacional (grant No.SIP-2024311).

References

Chen J., Ollis D.F., 1999, Kinetics processes of photocatalytic mineralization of alcohols on metallized titanium dioxide, Water Research, 33, 1173–1180.

Chiarello G. L., Ferri D., Selli E., 2018, In situ attenuated total reflection infrared spectroscopy study of the photocatalytic steam reforming of methanol on Pt/TiO_2, Applied Surface Science, 450, 146–154.

Downs R.T., Hall-Wallace M., 2003, The American Mineralogist Crystal Structure Database, The American Mineralogist Crystal Structure Database, 88, 247–250.

Fontelles O., Muñoz M. J., Conesa J. C., Kubacka A., Fernández M., 2018, H_2 photo-production from methanol, ethanol and 2-propanol: Pt-(Nb)TiO_2 performance under UV and visible light, Mol. Catal., 446, 88–97.

Li Z., Zhao M., Zeng J., Peng C., Wu J., 2017, High-solar-reflectance building ceramic tiles based on titanite ($CaTiSiO_5$) Glaze, Solar Energy, 153, 623–627.

Maeda K., 2011, Photocatalytic water splitting using semiconductor particles: history and recent developments, Journal Photochem Photobiol C - Photochem Reviews, 12, 237–68.

Mahanta U., Khandelwal M., Deshpande A.U. 2022, TiO_2@SiO_2 nanoparticles for methylene blue removal and photocatalytic degradation under natural sunlight and low-power UV light. Applied Surface Science, 576, Part A, 1, 151745

Muthuraman M., Patil K. C., 1998, Synthesis, properties, sintering and microstructure of sphene, $CaTiSiO_5$: a comparative study of coprecipitation, sol-gel and combustion process, Materials Research Bulletin, 33, 655–661.

O'Leary S. K., Lim P. K., 1997, On determining the optical gap associated with an amorphous semiconductor: A generalization of the Tauc model, Solid State Communications, 104, 17–21.

S. Onsuratoom, S. Chavadej, T. Sreethawong, 2011, Hydrogen production from water splitting under UV light irradiation over Ag-loaded mesoporous-assembled TiO_2–ZrO_2 mixed oxide nanocrystal photocatalysts, International Journal of Hydrogen Energy, 36, 5246-5261.

Stoyanova T., Matteucci F., Costa A.L., Dondi M., Ocana M., Carda J., 2017, Synthesis of Cr-doped $CaTiSiO_5$ ceramic pigments by spray drying, Solar Energy, 153, 623–627.

Udani P. P. C., Rønning M., 2015, Comparative study on the photo-catalytic hydrogen production from methanol over Cu-, Pd-, Co-and Au-loaded TiO_2, Oil & Gas Science and Technology, 70, 831–839.

Wang J.A., Limas R., Lopez T., Moreno A., Gomez R., Novaro O., Bohkimi X. 2001, Quantitative determination of titanium defects and solid state reaction mechanism in iron-doped TiO_2 photocatalysts, Journal of Physical Chemistry B 105, 9692–9698.

Zhu J., Zäch M., 2009, Nanostructured materials for photocatalytic hydrogen production, Current Opinion in Colloid & Interface Science, 14, 260–269.